

Lateral Current Injection Lasers: Underlying Mechanisms and Design for Improved High-Power Efficiency

Edward (Ted) H. Sargent, Genlin Tan, and Jimmy M. Xu

Abstract—The lateral current injection (LCI) laser—a promising technology for enabling optoelectronic integrated circuits and photonic devices with novel functionalities—is studied by comparison with conventional vertical injection devices. Fully self-consistent two-dimensional (2-D) simulations of lateral and vertical lasers reveal physical effects unique to the lateral injection class of devices. We find that 1) strong lateral carrier confinement is critical to efficient LCI laser operation, even if the active region is wide, in view of ambipolar effects, 2) current paths in parallel with the active region, even if they consist of high-bandgap intrinsic material, may nevertheless admit significant parasitic leakage even at moderate injection levels, and 3) a straightforward, but powerful, solution to the problem of premature roll-off in lasing efficiency may be achieved via heavy contact doping without significantly increasing modal free-carrier absorption.

Index Terms—OEIC's, optoelectronic integration, semiconductor device modeling, semiconductor lasers.

I. INTRODUCTION

WITH the benefit of countless iterations of experiment informed by continual improvements in theoretical understanding, edge-emitting semiconductor laser diodes have been fashioned which exhibit sub-mA threshold currents [1], double-ended differential quantum efficiencies in excess of 90% [2], and, recently, an extrapolated -3 dB modulation bandwidth under continuous wave (CW) operation of 43 GHz [3]. The benefits of high performance are offset by the disadvantage of design constraints which have resulted from principally one-dimensional structural development: the vertical dimension is the most elaborately variegated spatial degree of freedom in contemporary semiconductor lasers. Because structural variations may be so finely controlled during epitaxial growth, the principal axes of carrier flow, carrier capture, and optical mode confinement are parallel to the direction of growth. A consequence partly of technological considerations and partly of inertia, this limitation hinders flexibility of design and compatibility with multifunctional optoelectronic integration.

A family of semiconductor lasers which is less well understood than conventional vertical-injection (VCI) lasers, but

which possesses an intrinsic compatibility with optoelectronic integration as well as the potential to enable devices with new functionalities [4], is that of lateral current injection (LCI) lasers. LCI lasers may be grown on semi-insulating substrates and with highly resistive cladding layers for interdevice isolation and minimal free-carrier absorption. By inviting differentiation of the laser structure in the lateral direction as well as the vertical sense, lateral current injection liberates a new spatial degree of freedom for the development of novel, integrable devices. In the LCI laser, vertical and lateral device designs are fully or partially decoupled: for example, if the flow of carriers is in the direction parallel to the quantum wells, the vertical structure of multiquantum well active and cladding regions may be optimized for improved modal gain, modal differential gain, and far-field profile without hindering the transport of carriers.

The lateral current injection family of devices has so far achieved only moderate success through predominantly empirical trials [5]–[10]. The state of LCI laser theory has only recently progressed from virtual nonexistence to one in which a number of phenomena unique to LCI lasers have been identified: 1) an inherent asymmetry in the lateral carrier density distribution due to the electron-hole mobility disparity [11], [12], 2) a premature degradation in performance due to a reduction in the ambipolar diffusion length to a value much less than the contact spacing when high optical powers give rise to shortened recombination times [12], and 3) the often (though unintentionally) low degree of lateral carrier confinement in experimental structures [13]. An important factor whose effects remain to be studied quantitatively and in sufficient generality is the combined impact of higher current densities and larger voltage drops in LCI lasers compared to the traditional VCI devices.

There lacks a coherent, generalized perspective on the quantitative importance of the preceding effects in determining the performance of LCI lasers. We seek herein to address this shortcoming by considering in-depth the operation of a particular set of laser structures which are technologically interesting and physically revealing. We apply fully self-consistent two-dimensional (2-D) finite-element simulation to laser diodes of the VCI and LCI paradigms. By studying the better understood VCI family at the same time, we provide a benchmark relative to which we may assess our new insights into the essential physical mechanisms governing the operation of OEIC-compatible lateral current injection lasers.

Manuscript received February 25, 1998. This work was supported by the Ontario Centre for Materials Research, Nortel Technology, and the National Sciences and Engineering Research Council of Canada.

The authors are with the Department of Electrical and Computer Engineering, University of Toronto, Toronto, Ont., M5S 1A4 Canada.

Publisher Item Identifier S 0733-8724(98)07401-5.

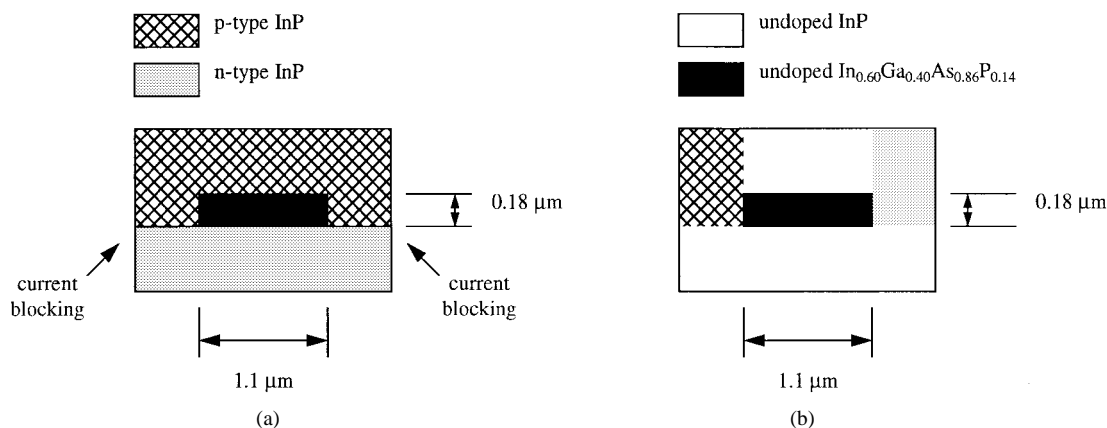


Fig. 1. Semiconductor laser structures considered in this work. The (a) vertical and (b) lateral current injection laser studied have identical active region composition and volume, electrical and optical materials parameters, and contact and background doping levels. Only the placement of doped regions and contacts is changed.

II. METHOD

We consider herein the case of related semiconductor lasers operating at $1.3 \mu\text{m}$. We have chosen a simple bulk active region laser because the structural simplicity of the device lends itself to a distillation of the fundamental physical effects which we wish to highlight; because experimental reports are available for similar devices in both the VCI [14] and LCI [10] paradigms; and because while there are clearly important differences between bulk and technologically more important quantum-well lasers, our findings translate at a qualitative level from the former case to the latter. If the LCI laser design principles which we elaborate herein are applied to multiquantum well structures, the benefits of low threshold carrier density and suppressed Auger recombination may be realized, leading to further improvements in device characteristics.

The device structure considered is illustrated schematically in Fig. 1. We indicate in the Appendix that the known or assumed materials properties [15] of the lasers whose operation is treated herein. The vertical injection laser of Fig. 1(a) is of the buried-heterostructure type; a current blocking mechanism (e.g., p-n-p-n structure) prevents current from circumventing the active region. It was found previously that current leakage in such a laser is instead dominated by overbarrier leakage of electrons from within the active region [16]. In contrast, the minimally doped top cladding layer of the LCI laser of Fig. 1(b) represents a potential leakage path under high forward bias. We discuss in Sections III and IV the consequences of these assumptions and address therein the important issue of carrier leakage around the active region of the LCI laser as well as considering overbarrier leakage in both devices.

We study physical device operation by solving self-consistently Poisson's equation, the electron and hole continuity equations, the optical wave equation, and the photon rate equation in two dimensions [17]. We include in our model spontaneous, stimulated, Shockley-Read-Hall, and Auger recombination. In order to facilitate comparison with previous studies of conventional VCI lasers, we use the gain-carrier density relationship [16], [18] indicated

in the Appendix. We include loss associated with intraband absorption in addition to mirror loss.

We have refrained from introducing phenomenological factors—for example, “scattering loss” or “intrinsic loss,” or Auger recombination coefficients higher than those usually obtained by measurement—which are often added in an attempt to achieve agreement between theoretical predictions and experimental measurements of threshold current and lasing efficiency. As a result, our quantitative results are optimistic, appropriate only under idealized conditions. However, all of our conclusions are derived by comparing the operation of VCI and LCI lasers simulated under an identical set of assumptions. Our qualitative findings are therefore informative, and comparison with experiment could readily be made by a simple scaling from the ideal to the real case by *post facto* introduction of the requisite phenomenological factors.

As evidenced in the following section, a number of competing intrinsically 2-D effects which distinguish the VCI and LCI devices, and which would not have been brought out by a model that was either one-dimensional (1-D) or not fully self-consistent, were revealed using this approach.

III. RESULTS

We begin by reporting on the output measures of practical significance: relationships between current, voltage, and output optical power. Fig. 2 shows the calculated optical output per facet, differential quantum efficiency, voltage, and differential resistance, all as a function of current, for the vertical and lateral devices. Differences in these results between the two devices immediately raise a number of issues meriting in-depth investigation.

A. Higher Initial Efficiency in Lateral Current Injection Laser

The higher initial differential quantum efficiency in the LCI laser is a consequence of a difference in modal free carrier absorption between the lateral and vertical devices. The fraction of the optical mode which overlaps with the doped contact/cladding regions is ten times greater in the vertical injection case than in the lateral case. This arises because the vertical dimension of the high index region is usually

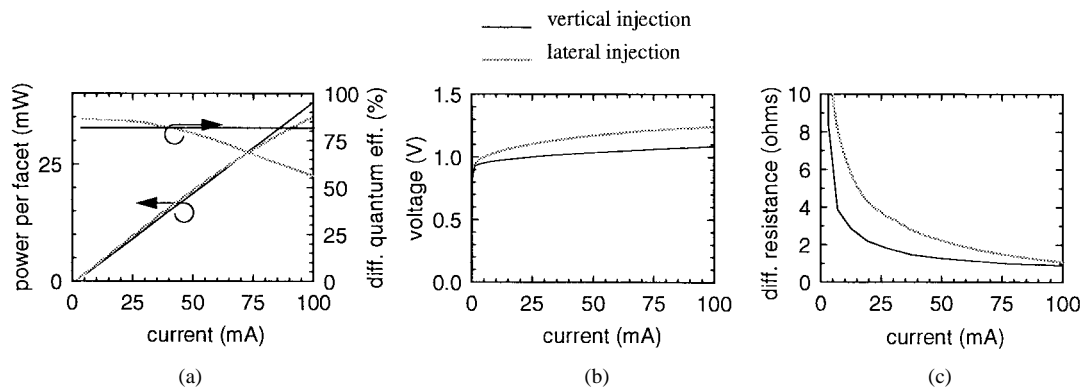


Fig. 2. (a) Optical power output per facet and total differential quantum efficiency, (b) voltage, and (c) differential resistance of vertical and lateral current injection lasers.

substantially less than an optical half-wavelength inside the medium, whereas the lateral dimension is generally much greater. In the structures considered, the component of modal free carrier absorption due to the contact regions is ten times higher as a result. The differential optical output efficiency is proportional to $\alpha_m/\alpha_m + \alpha_i$, where α_m is the mirror loss and α_i accounts for other loss effects such as scattering and free-carrier absorption. Intraband absorption is responsible for the difference in calculated initial quantum efficiency seen in Fig. 2(a).

Irrespective of the quantitative importance of this initial efficiency improvement, the preceding results highlight one important general feature of the LCI family of devices. When a new spatial degree of freedom is released, a number of design features which are mutually constraining in the vertical injection case become decoupled in the lateral case. In the vertical injection paradigm, the direction of current injection and of tightest optical confinement are the same and the optical mode therefore overlaps vertically with regions of heavily doped cladding material. In the lateral injection case, the direction of injection and of tightest confinement are orthogonal, and the resulting design flexibility affords the possibility of creating a device with a greater initial differential quantum efficiency and lower capacitance.

A number of similar benefits arise when consideration is extended to more advanced laser devices. For example, the mode-confining SCH region of an LCI multiquantum-well laser may be engineered to be essentially free of carriers, affording reduced free-carrier absorption and associated wavelength chirp under direct modulation. In addition, since carriers in the LCI laser are injected directly from heavily doped contacts into the quantum wells, the frequency-damping effects associated with ambipolar drift-diffusion in the SCH of a vertical injection laser [19] may be reduced.

B. Lower Differential Efficiency Under High Bias

It was shown previously [12] that LCI lasers whose contact separations exceed their carrier ambipolar diffusion length exhibit a lateral carrier distribution asymmetry which leads to a reduced overlap between the optical mode profile and the local material gain distribution. It was further seen that at high optical powers, the increased rate of stimulated emission

gives rise to a further decrease in the ambipolar diffusion length, reduced mode-gain overlap, and a further deterioration in differential quantum efficiency.

We may envisage a number of physical effects which could conspire to reduce the differential quantum efficiency in lateral injection lasers. We describe these and then proceed to consider their relative importance.

1) *Reduced Lateral Gain-Mode Overlap:* As the recombination time decreases with increasing optical power, the degree of lateral carrier density asymmetry increases. Because holes are generally much heavier than electrons in unstrained III-V semiconductor materials, the peak of the lateral carrier distribution is at the P-i junction. In contrast, the maximum of the lateral optical mode distribution is in the lateral middle of the intrinsic active region. This effect is illustrated in Fig. 3, in which carrier density (to which the local optical gain is taken to be proportional in the bulk active region laser considered) is plotted against lateral position for increasing output powers. Whereas the carrier and gain distributions change with increasing current, the optical mode profile remains fixed in strongly index-guided devices.

2) *Superlinear Dependence of Recombination Rate on Carrier Density:* Because the asymmetry of the carrier density distribution grows with increasing optical power, the higher moments of the carrier density distribution would increase even if the average carrier density were to remain constant. As a result, recombination mechanisms characterized by super-linear dependencies on the local carrier density—mechanisms which include bimolecular (spontaneous) and Auger recombination—contribute to higher “parasitic” recombination currents in the device.

3) *Sublinear Gain-Carrier Density Dependence:* A third factor occurs in devices whose active regions exhibit a sublinear dependence of gain on carrier density. In a bulk active region laser with an approximately linear gain-carrier density relationship, if the optical intensity were approximately constant over the width of the active region, then as the carrier density nonuniformity increased above threshold, a constant average carrier density would be sufficient to maintain zero net round-trip gain. However, in a quantum-well laser with a sublinear gain-carrier density relationship, a more nonuniform lateral carrier density distribution would

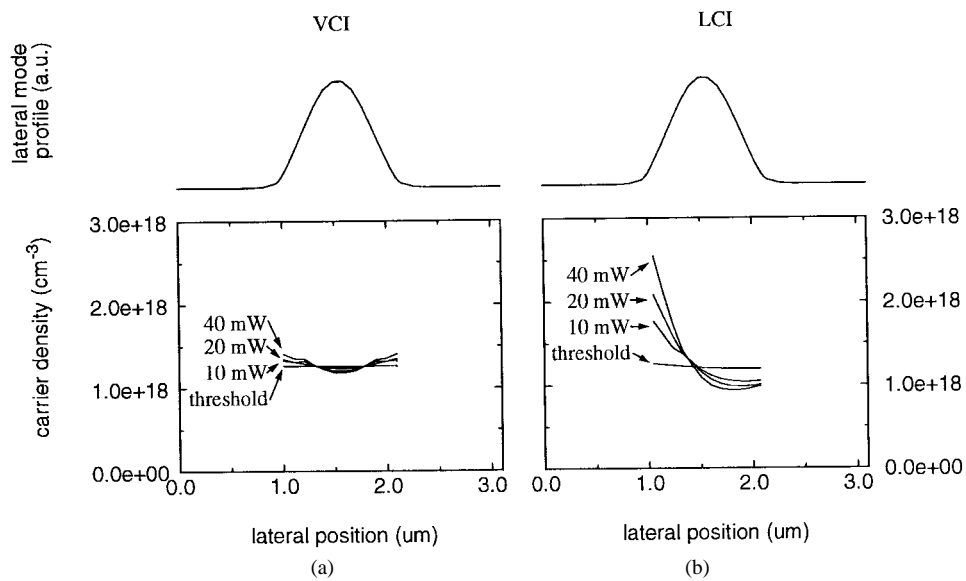


Fig. 3. Evolution of lateral carrier density profile required to sustain lasing oscillation in (a) vertical injection and (b) lateral injection devices. The lateral mode profile is shown in order to indicate both the origins of the spatial hole burning in each device and also to suggest the reduction in the overlap integral between the local gain and optical mode profile which constitutes the modal gain.

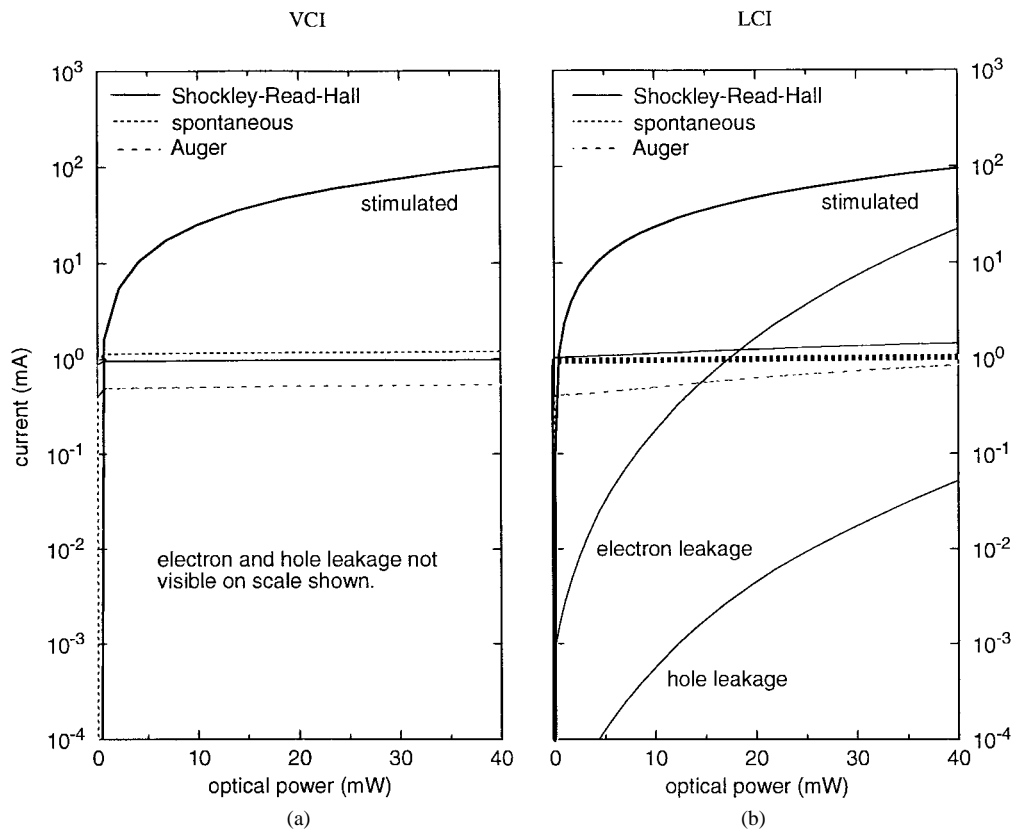


Fig. 4. Development of recombination and leakage components of current with increasing output optical power for (a) vertical and (b) lateral current injection devices.

necessitate an increased average carrier density in order to sustain lasing oscillation.

The importance of the first two effects as a function of optical power is revealed in Fig. 4 for the vertical and lateral injection lasers. The vertical injection laser exhibits approximate “carrier density pinning” above threshold; a small deviation from this (indicated by the slight increase in recom-

binations current components with increasing optical power) is a consequence of mild spatial hole burning, illustrated in Fig. 3(a).

There is a more pronounced increase in the total rate of nonstimulated recombination in the case of the lateral injection laser [Fig. 4(b)] as a consequence of the increased carrier density nonuniformity [Fig. 3(b)]. Since the rate of

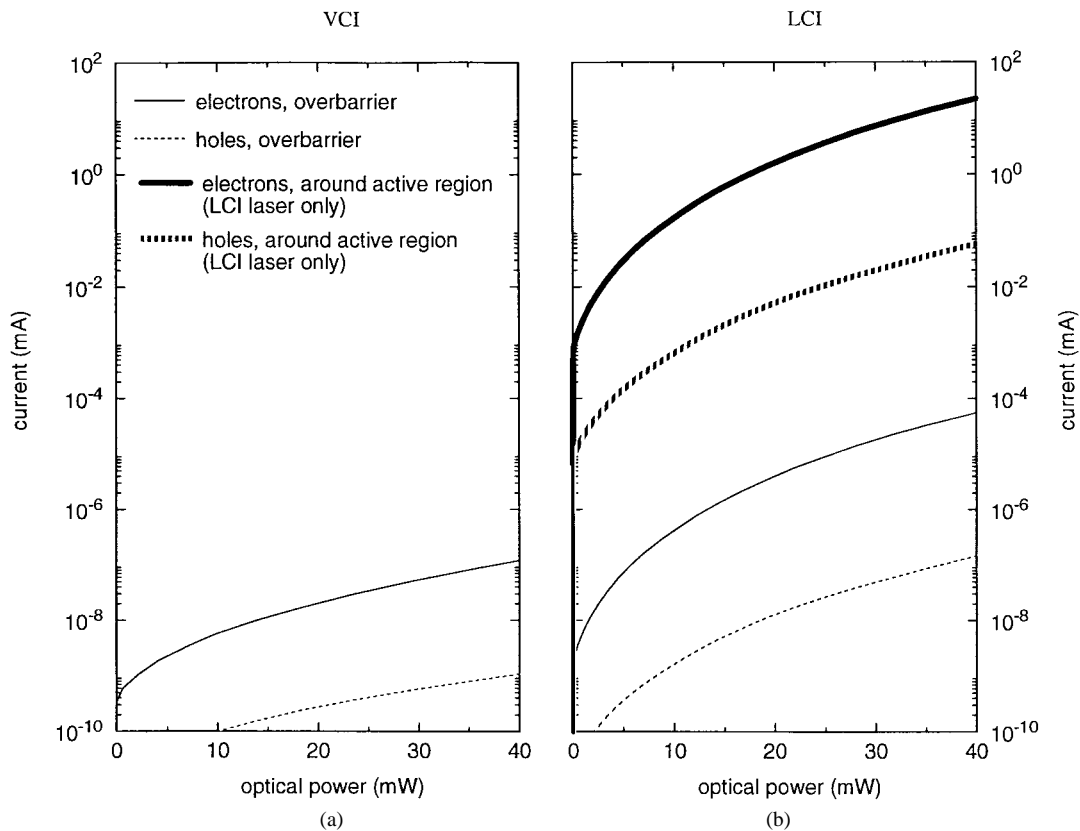


Fig. 5. Breakdown of leakage current components in (a) vertical and (b) lateral injection lasers in terms of whether carriers are injected into the active region and then suffer overbarrier leakage, or whether they circumvent the active region altogether.

Shockley–Read–Hall recombination is proportional to the carrier density, the increase in SRH recombination current with optical power indicates that the average carrier density in the active region is increasing above threshold. This is symptomatic of the first effect described above wherein reduced overlap between the lateral spatial profiles of local gain and fundamental optical mode necessitates an increase in the total number of carriers in the active region if lasing is to be sustained.

In view of the superlinear dependence of their recombination rates on the local carrier density, currents associated with spontaneous and Auger processes increase at a faster rate than the SRH recombination current [Fig. 4(b)]. Their increase is a consequence of the combination of reduced mode-gain overlap and increased higher order moments (e.g., in the case of spontaneous recombination) associated with a more nonuniform carrier density distribution.

The mechanisms described above account for a relatively slow initial roll-off in differential quantum efficiency shown in Fig. 2(a) for the LCI laser. A change in the rate of efficiency roll-off occurs at higher currents and suggests that a new efficiency-decreasing mechanism takes over. It is seen in Fig. 4(b) that this mechanism is an increased flux of leakage electrons into the p -contact, following which the electrons recombine nonradiatively with holes in the bulk semiconductor or at the metal-semiconductor contact.

In the LCI laser considered, carrier leakage may be such that carriers circumvent the active region entirely, flowing

through the forward-biased $P(\text{InP}, 2E18 \text{ cm}^{-3}) - N(\text{InP}, 1E15 \text{ cm}^{-3})$ junction in the cladding material; or such that {electrons, holes} present in the active region, but not yet recombined, are caused to overflow into the {P, N} contacts. Because the LCI laser does not incorporate a current-blocking mechanism, leakage around the active region, rather than overbarrier leakage of carriers already captured into the active region, dominates the leakage current contribution, as seen in Fig. 5. This parasitic effect is made more severe in the LCI laser for two reasons: 1) a large voltage is required to achieve a given output power, as seen in Fig. 2(a) and (b) and 2) the ratio of the cross-sectional area of exposed active region to the cladding leakage path area is much less than unity.

From the preceding analysis it is clear that in the devices considered herein, the principal source of performance deterioration at high injection levels in the LCI relative to the VCI device lies in a difference in parasitic leakage currents. Since the severity of this effect is closely linked to the higher resistance of the lateral injection device, and in view of the role of the voltage-current relation in governing device heating, we now proceed to examine the physical origins of voltage accumulation in the vertical and lateral injection lasers.

C. Underlying Physical Origins of Current-Voltage and Leakage Characteristics

We show in Fig. 6 band diagrams at zero bias, threshold, and 40 mW/facet output power for the VCI and LCI lasers. It is clear from examination of Fig. 6 that an appreciable portion

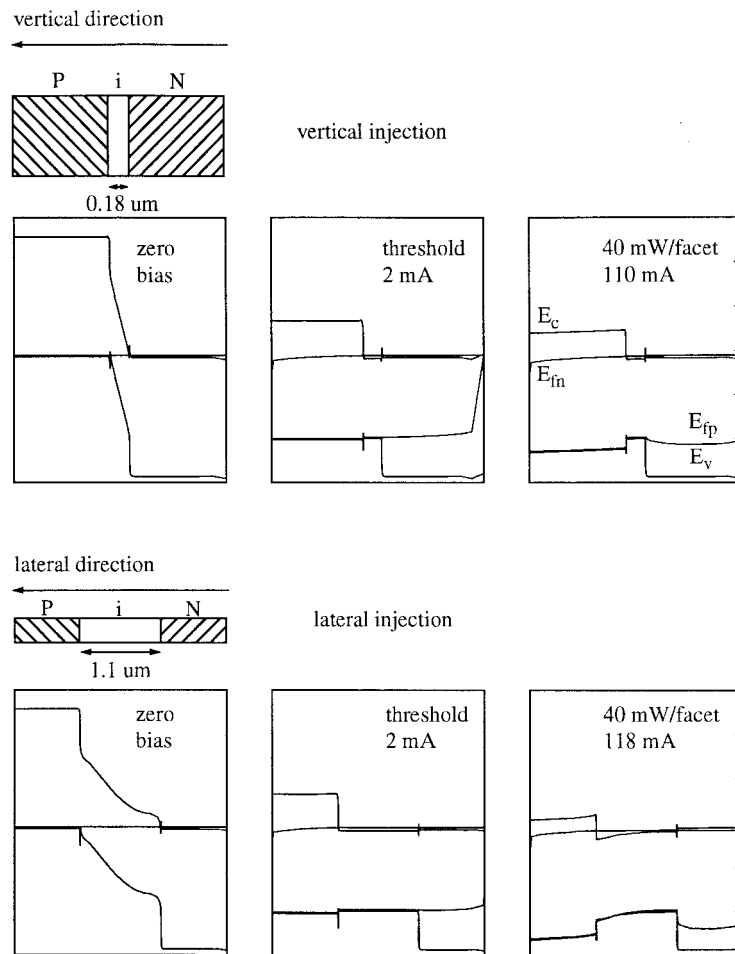


Fig. 6. Band diagrams for vertical and lateral injection lasers at zero bias, threshold current, and at 40 mW/facet output power.

of the differential bias applied in the evolution from threshold to 40 mW/facet output power lies across the intrinsic active region of the device, while this effect is much smaller in the VCI case.

Also evident in the band diagrams is a difference in the rate of increase of the potential across the depleted p-i heterojunction (a vertical junction in the VCI case and a lateral one in the LCI case) under increasing bias current. As the density of current passing over a heterojunction rises, the voltage drop across the depletion layer also increases. This voltage accumulation, which occurs principally at the p-side barrier, increases essentially as the logarithm of current density for large current densities (see, for example, [16]). For the same *current* injected into the active region, the *current density* in the LCI laser active region considered is about six times greater than in the VCI laser because of the sixfold decrease in the cross-sectional area available for injection in the LCI case. In view of the preceding logarithmic relation, we expect the differential resistance associated with this voltage accumulation to be somewhat less than twice that of the vertical injection laser. A further source of differential resistance lies in the buildup of voltage across bulk semiconductor contacts or tubs.

Having presented these effects qualitatively, we wish now to determine which have the greatest impact on the operation

of real devices. To quantify these effects, we divide each laser into segments across which we monitor the applied voltage as a function of current as indicated in Fig. 7. In Fig. 8, we follow the evolution of these additive voltage components with current; in Fig. 9, we focus in on the derivative of the quantities of Fig. 8, namely, the series component differential resistances. In calculating and plotting the component differential resistances of Fig. 9, we use not the total current, but instead the current injected into the active region. In this way we isolate voltage and leakage effects. (Calculating differential resistance in terms of total, rather than injected, current would mislead by suggesting an artificially low differential resistance in the LCI laser case in view of its more severe leakage effects.) The differential resistances treated herein may therefore be considered to appertain to the active region in isolation from its surrounding, potentially leaky, cladding layers.

For both vertical and lateral lasers, the voltage across the N-i heterojunction is constant above threshold; in contrast, the voltage across the P-i heterojunction rises much more rapidly in the LCI laser case than the vertical injection case. The voltage drop across the active region of the VCI laser is very nearly pinned above threshold while it continues to grow above threshold in the LCI case. These issues are further brought out if we consider the differential resistance curves.

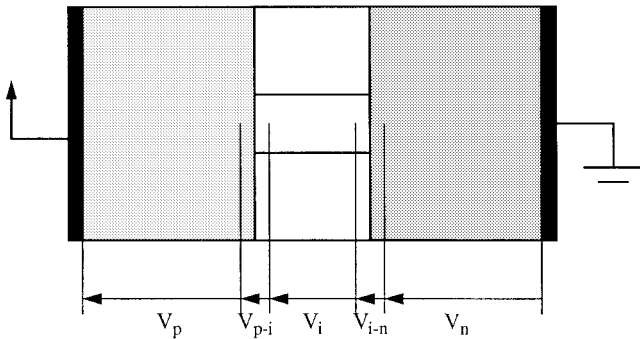


Fig. 7. Division of voltage drops across a laser (either vertical or lateral) into components associated with bulk majority carrier resistive flow (V_p, V_n) current-dependent heterojunction voltage drops (V_{p-i}, V_{i-n}), and ambipolar drift-diffusion (V_i).

The continued development of the P-i heterojunction potential dominates the differential resistance of the VCI laser, while the combination of this potential plus that across the active regions is responsible for the higher differential resistance in the LCI laser case. As expected, the LCI laser P-i heterojunction differential resistance is typically less than twice that of the vertical injection case; the $(dV/dI) \propto (1/I)$ dependence is a consequence of the logarithmic dependence of junction voltage on current discussed above.

The gradual decrease in the resistance of the active region itself is a consequence of the increase in the average carrier density in the active region with increasing bias. The differential resistance above threshold in a region in which ambipolar diffusion dominates is given approximately by the expression [20]

$$R_i = \frac{L_{\text{path}}}{\text{Area}} \frac{1}{q(\mu_n + \mu_p)n}. \quad (1)$$

As the bias increases, gain-mode overlap deteriorates, a higher average is needed to sustain laser oscillation, and the differential resistance of the LCI laser decreases gradually.

Also worthy of comparison are the quantitative differential resistance values associated with bulk conduction through the P-contact. Close to the metallic contact and far from the active region, the cross-sectional P-contact area seen in the vertical and lateral injection cases are similar. On the other hand, at the active region itself, the cross-sectional area for injection is approximately six times less for the LCI laser considered. This current constriction effect accounts for the approximately two times larger differential resistance associated with the P-contact in the LCI laser case compared to the VCI case.

IV. DISCUSSION

The preceding results point to useful generalizations as to the operation and performance of LCI lasers. By choosing a device structure with an active region which was both thick and narrow, we succeeded in keeping those effects associated with reduced mode-gain overlap to an acceptably low level. Some previous experimental LCI laser trials [5]–[10] have suffered more severely from such effects because they employed either 1) active regions which were much wider than the ambipolar diffusion length or 2) active regions which

were so thin and which had such a low total confinement factor that a high average carrier concentration was needed to sustain lasing operation, giving rise in turn to a very short recombination time and reduced ambipolar diffusion length.

With carrier density asymmetry and nonpinning effects kept under control, we found that another effect—leakage around the active region—was the dominant source of a moderate performance roll-off at high biases. This leakage mechanism is characterized by the turn-on voltage of the parasitic p-i-n diode which is in turn a function of the bandgap of the leaking material (InP in the case considered). This leakage mechanism in the LCI laser considered was particularly severe 1) because of its higher resistance (due mainly to higher P-i junction and intrinsic active region differential resistances) such that for a given current through the active region a higher voltage appeared across the parallel leakage path and 2) because of the larger ratio of leakage path cross-section to active region cross-section in the LCI laser.

These predictions as to the expected behavior of LCI lasers are confirmed by comparison with experimental results. For example, in a study of lasers with differing contact spacings (1.5 and 4.5 μm) but otherwise identical structures [10], the threshold current was increased by a factor greater than the fractional increase in active region volume, and the pulsed-mode differential quantum efficiency rolled off at much lower optical powers in the case of the wider device. This marked difference in the performance of the otherwise identical devices may be attributed to the importance of carrier density nonpinning effects in the device whose active region width exceeded the carrier ambipolar diffusion length. Another experimental LCI laser [5], this one with a narrow active region (0.5 μm wide), achieved higher power operation since it did not suffer the same carrier density asymmetry effects. Its pulsed-mode lasing efficiency nevertheless deteriorated above 60 mA. The highly reported series resistance for this device would imply that a large voltage had accumulated by this point across the thick cladding region parasitic path, giving rise to the observed roll-off in pulsed-mode efficiency. Another experimental device [21], this one incorporating doped current guiding layers above and below the active region for “hybrid” current injection, motivated an in-depth examination [11] of its more complex leakage effects. In sum, it would appear that two of the physical effects considered in this work—carrier density asymmetry and current density/voltage accumulation phenomena—have indeed been manifest in previous reported experimental works.

Having revealed through a combination of theory and experiment the qualitative and quantitative importance of these mechanisms, we may consider ways in which to rectify the leakage problem. First, we may reduce the total LCI laser device resistance. This has the benefit of reducing the leakage current as well as the resistive heating, the latter factor having revealed its importance in experimental comparisons of continuous wave versus pulsed L-I characteristics [5]–[10]. The LCI laser resistance was seen in Fig. 9(b) to be a result predominantly of P-i heterojunction voltage build-up

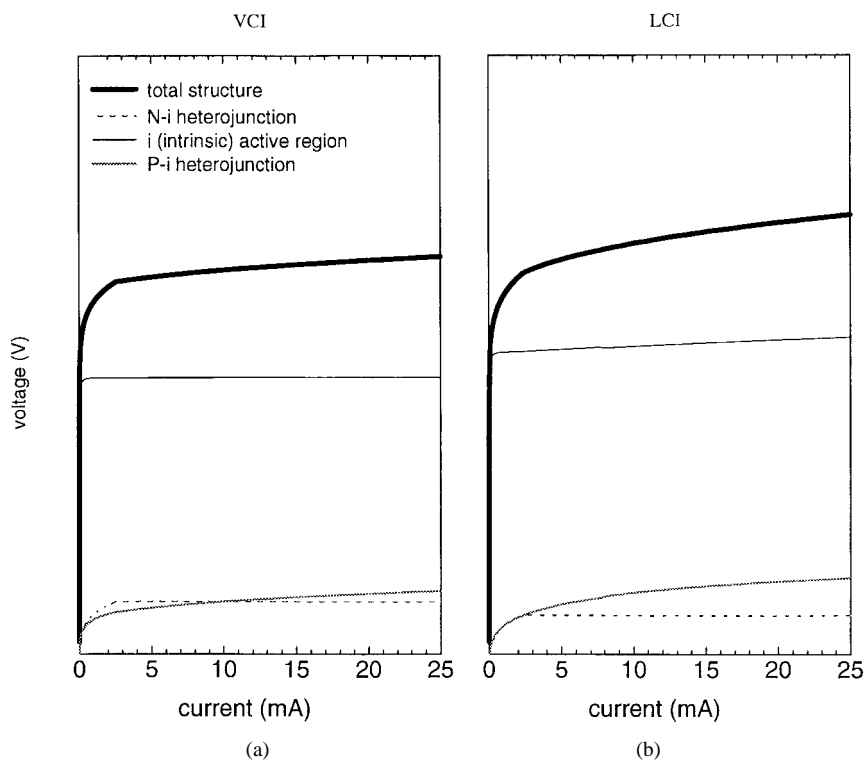


Fig. 8. Development of voltage drops and components thereof as a function of current injected into the active region. Results are obtained for (a) vertical and (b) lateral injection devices.

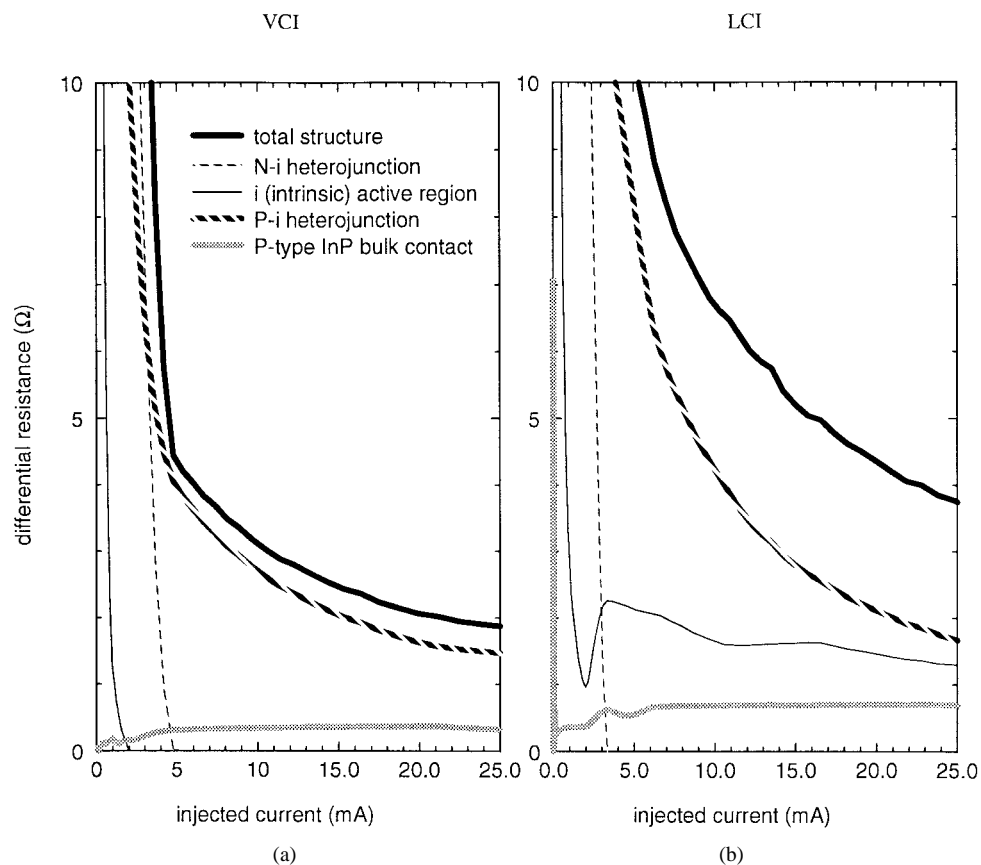


Fig. 9. Differential resistance and components thereof as a function of current injected into the active region. Results are obtained for (a) vertical and (b) lateral injection devices.

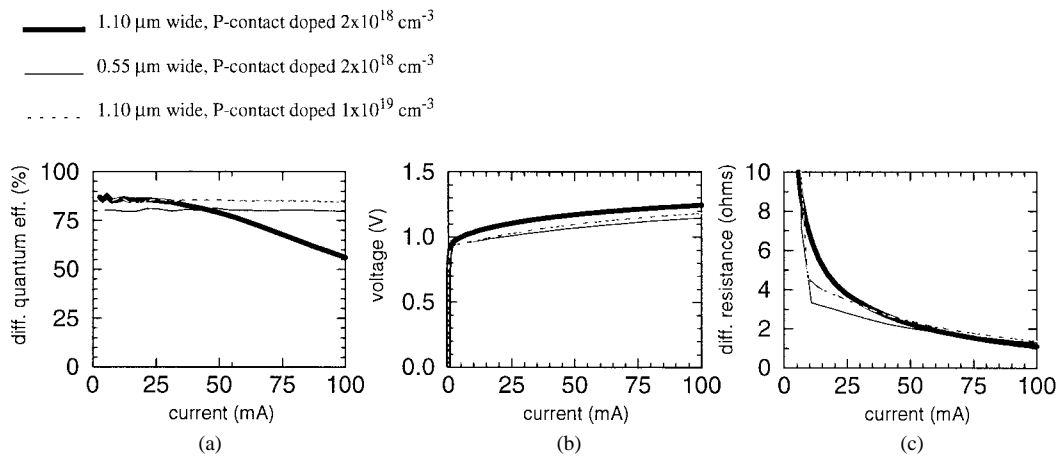


Fig. 10. (a) Differential quantum efficiency, (b) voltage, and (c) differential resistance of three different LCI lasers. Thick continuous lines denote the LCI laser considered previously herein; thin continuous lines refer to this same device with its active region width reduced by a factor of two; and thin broken lines refer to the same device as considered previously, with the original active region width of $1.1 \mu\text{m}$, but with the p-contact much more heavily doped at $1 \times 10^{19} \text{ cm}^{-3}$. It is seen that the leakage problem revealed in this work is effectively addressed using either the active region narrowing or the P-contact doping approach.

combined with the ambipolar differential resistance of the active region.

The rate of voltage accumulation across the P-i heterojunction may be slowed by increasing the doping of the P-contact, as derived analytically in [16]. The critical features is the doping right at the heterojunction (effectively within a Debye length of the heterojunction), so that the approach sometimes employed in vertical injection lasers of a downward grading of the doping as the heterojunction is approached would not achieve the purpose of lowering this resistive contribution. Fortunately, the optical mode will usually be well confined in the lateral direction, so that there is only a small degree of overlap between the lateral optical mode profile and the region of proposed heavy doping.

The intrinsic active region resistance may be lowered by increasing carrier mobility and decreasing the length of the conduction path [see (1)]. Mobility improvements may be achieved by the use of a strain-compensated multiquantum well active region in which the heavy hole—light hole mass degeneracy is broken, resulting in reduced heavy-hole effective mass [22]. Path length may be reduced to within the practical lithographic limitations.

We show in Fig. 10 simulation results from our study of a laser with a heavily doped p-contact and an active region width of $0.55 \mu\text{m}$, a width regime accessible via precise optical lithography. Either of these solutions gives rise to an essentially flat differential efficiency above threshold up to 100 mA current, as well as reduced bias voltages and differential resistances.

Another approach to reducing the effects of leakage current which circumvents the active region is to increase the resistance of the parasitic path. This may be achieved either by doping InP with Fe in order to introduce traps which inhibit conduction, or by using a wider bandgap cladding material (such as oxidized semiconductor or dielectric). An additional approach is to regrow contacts such that electrical contact is made solely to the active region and not to the parasitic path responsible for lateral leakage, thereby reducing the effective cross-sectional area for leakage.

V. CONCLUSIONS

Aided by self-consistent simulations of vertical and lateral injection lasers, we have arrived at a number of new insights into the physics and design of LCI lasers.

- 1) It might seem on first consideration that with injecting contacts separated by a distance on the order of an ambipolar diffusion length, most electrons and holes would recombine in the active region even without the benefit of carrier-confining heterojunctions. In fact, in the ambipolar regime, high-mobility electrons readily reach the opposite contact and electron leakage will be severe unless strong carrier confinement is introduced.
- 2) It might appear that with high-bandgap intrinsic material in parallel with the LCI laser active region, parallel leakage through cladding layers should be minimal. This is true at threshold, where the voltage applied across the active region and parasitic paths is slightly greater than that corresponding to the active region bandgap. However, because of higher current densities in LCI lasers, the above-threshold differential resistance of the active region is typically much higher than in vertical lasers. For this reason, voltage may rapidly accumulate across the parasitic path above the lasing threshold so that parallel leakage causes the lasing efficiency to drop drastically at low or moderate powers.
- 3) Since p-n-p-n current blocking structures are not readily realized in the lateral injection scheme, other solutions to the leakage problem must be found. Perhaps paradoxically, one straightforward but powerful solution to the problem of early leakage onset is to increase the contact doping. At first this might seem ineffective, for it increases access to both carrier paths (both active region injection as well as parallel leakage) equally. In fact, since increasing the contact doping lowers the heterojunction differential resistance under high injection, the total active region differential resistance is reduced and the onset of substantial parallel leakage postponed.
- 4) It might appear that the strategy frequently adopted in vertical injection laser design of grading doping

TABLE I

Quantity	Value
Electron intraband absorption	$\alpha_{\text{electron}} = (3 \times 10^{-18} \text{ cm}^2) \times n$
Hole intraband absorption	$\alpha_{\text{hole}} = (7 \times 10^{-18} \text{ cm}^2) \times p$
Material gain	$g(n) = 2.5 \times 10^{-16} \text{ cm}^2 \times (n - 8 \times 10^{17} \text{ cm}^{-3})$
Electron mobility	$3500 \text{ cm}^2/\text{Vs}$
Hole Mobility	$200 \text{ cm}^2/\text{Vs}$
n-type background doping	$1 \times 10^{15} \text{ cm}^{-3}$
P-contact doping	$2 \times 10^{18} \text{ cm}^{-3}$
N-contact doping	$2 \times 10^{18} \text{ cm}^{-3}$
Shockley-Read-Hall Recombination time	10 ns
Spontaneous recombination rate	$R_{\text{spont}} = (0.9 \times 10^{-10} \text{ cm}^3 \text{ s}^{-1}) np$
Auger recombination rate	$R_{\text{spont}} = (2.95 \times 10^{-29} \text{ cm}^6 \text{ s}^{-1}) \left(\frac{n^2 p + n p^2}{2} \right)$

downward from high to moderate levels as the active region is approached could usefully be applied in LCI lasers. In fact, this is not only unnecessary, but also does not aid in resolving the leakage problem. It is not necessary because heavy doping right at the heterojunction between the p-contact and the active region will not give rise to intolerable modal free-carrier absorption in view of the minimal confinement of the lateral mode to the lateral contacts. It is not helpful because, for the differential resistance of the heterojunction to be usefully reduced, heavy doping must exist within a Debye length of the junction.

With the benefit of further experimental trials informed by continued improvements in the theoretical understanding of the physical mechanisms which underlie lateral current injection laser operation, we foresee increased realization of the tremendous potential of the LCI laser. This may in turn open up new directions in optoelectronics, just as explorations of the lateral direction in electronics contributed to the realization of practical electronic integrated circuits.

APPENDIX

MATERIAL AND STRUCTURAL PARAMETERS

See Table I.

REFERENCES

- [1] T. R. Chen, L. E. Eng, B. Zhao, Y. H. Zhuang, and A. Yariv, "Strained single quantum well InGaAs lasers with a threshold current of 0.25 mA," *Appl. Phys. Lett.*, vol. 63, pp. 2621–2623, 1993.
- [2] S. H. Groves, J. N. Walpole, and L. J. Missaggia, "Very high efficiency GaInAsP/GaAs strained-layer quantum well lasers ($\lambda = 980 \text{ nm}$) with GaInAsP optical confinement layers," *Appl. Phys. Lett.*, vol. 61, pp. 255–257, 1992.
- [3] X. Zhang, A. Gutierrez-Aitken, D. Klotzkin, P. Bhattacharya, C. Caneau, and R. Bhat, "0.98- μm multiple-quantum-well tunneling injection laser with 98-GHz intrinsic modulation bandwidth," *IEEE J. Select. Topics Quantum Electron.*, vol. 3, pp. 309–314, 1997.
- [4] E. H. Sargent, G. L. Tan, and J. M. Xu, "Physical model of OEIC-compatible lateral current injection lasers," *IEEE J. Select. Topics Quantum Electron.*, vol. 3, pp. 507–512, 1997.
- [5] A. Furuya, M. Makiuchi, O. Wada, and T. Fujii, "AlGaAs/GaAs lateral current injection multi-quantum well (LCI-MQW) laser using impurity-induced disordering," *IEEE J. Quantum Electron.*, vol. 24, pp. 2448–2453, 1988.
- [6] Y. Honda, I. Suemune, N. Yauhira, and M. Yamanishi, "Continuous-wave operation of a lateral current injection ridge waveguide AlGaAs/GaAs laser with a selectively-doped heterostructure," *Japan J. Appl. Phys.*, vol. 30, pp. 990–991, 1991.
- [7] J. Ohta, K. Kuroda, K. Mitsunaga, K. Kyuma, K. Hamanaka, and T. Nakayama, "Buried transverse-junction stripe laser for optoelectronic-integrated circuits," *J. Appl. Phys.*, vol. 61, pp. 4933–4935, 1987.
- [8] W. Yang, A. Gopinath, and M. Hibbs-Brenner, "Planar GaAs-AlGaAs MQW transverse junction ridge waveguide lasers using shallow zinc diffusion," *IEEE Photon. Technol. Lett.*, vol. 7, pp. 848–850, 1995.
- [9] Y. Kawamura, Y. Noguchi, and H. Iwamura, "Lateral current injection InGaAs/InAlAs MQW lasers grown by GSMBE/LPE hybrid method," *Electron. Lett.*, vol. 29, pp. 102–104, 1993.
- [10] Y. Suzuki, S. Mukai, H. Yajima, and T. Sato, "Transverse junction buried heterostructure (TJ-BH) AlGaAs diode laser," *Electron. Lett.*, vol. 23, pp. 384–385, 1987.
- [11] D. A. Suda, H. Lu, T. Makino, and J. M. Xu, "An investigation of lateral current injection laser internal operation mechanisms," *IEEE Photon. Technol. Lett.*, vol. 7, pp. 1122–1124, 1995.
- [12] E. H. Sargent and J. M. Xu, "Investigation of the physical mechanisms governing the performance of OEIC-compatible *p-i-n* active region lateral injection lasers," in *Proc. 9th Annu. Meeting, IEEE Lasers Electro-Opt. Soc. (LEOS)*, 1996.
- [13] ———, "Integration-compatible lateral current injection lasers: Design of 2-D heterostructure devices," in *Proc. Conf. Lasers Electro-Opt. (CLEO)/Pacific Rim*, 1997.
- [14] P. A. Andrekson, R. F. Kazarinov, N. A. Olsson, T. Tabun-Ek, and R. A. Logan, "Effect of thermionic electron emission from the active layer on the internal quantum efficiency of InGaAsP lasers operating at 1.3 μm ," *IEEE J. Quantum Electron.*, vol. 30, pp. 219–221, 1994.
- [15] P. Bhattacharya, Ed., *Properties of Lattice-Matched and Strained Indium Gallium Arsenide*. London, U.K.: INSPEC, the Institution of Electrical Engineers (IEE), 1993.
- [16] R. F. Kazarinov and M. R. Pinto, "Carrier transport in laser heterostructures," *IEEE J. Quantum Electron.*, vol. 30, pp. 49–53, 1994.
- [17] G.-L. Tan, N. Bewtra, K. Lee, and J. M. Xu, "A two-dimensional non-isothermal finite element simulation of laser diodes," *IEEE J. Quantum Electron.*, vol. 29, pp. 822–835, 1993.
- [18] G. P. Agrawal and N. K. Dutta, *Semiconductor Lasers*. New York: Van Nostrand Reinhold, 1993.
- [19] S. C. Kan, D. Vassilovski, T. C. Wu, and K. Y. Lau, "On the effects of carrier diffusion and quantum capture in high speed modulation of quantum well lasers," *Appl. Phys. Lett.*, vol. 61, pp. 752–754, 1992.
- [20] A. Herlet, "The forward characteristic of silicon power rectifiers at high current densities," *Solid State Electron.*, vol. 11, pp. 717–742, 1968.
- [21] K. Oe, Y. Noguchi, and C. Caneau, "GaInAsP lateral current injection lasers on semi-insulating substrates," *IEEE Photon. Technol. Lett.*, vol. 6, pp. 479–481, 1994.
- [22] E. Yablantovitch and E. O. Kane, "Reduction of lasing threshold current density by lowering of valence band effective mass," *J. Lightwave Technol.*, vol. LT-4, pp. 504–507, 1986.

Edward (Ted) H. Sargent receiving the B.Sc. degree in engineering physics from Queens University, Kingston, Ont., Canada, in 1995 and the Ph.D. degree in photonics from the University of Toronto, Toronto, Ont., Canada, in 1998.

Currently, he holds the Nortel Junior Chair in Emerging Technologies in the Department of Electrical and Computer Engineering, University of Toronto. He has authored over 20 contributed papers and given more than ten invited papers. As part of his Doctoral dissertation, "The Lateral Current Injection Laser: Theory, Design, Fabrication," he and Prof. Xu developed the first theory of this device for enabling optoelectronic integrated circuits and functional devices, developed improved lateral injection laser designs, and fabricated and characterized exploratory devices. While a student at the University of Toronto, he was sponsored variously by the Ontario Centre for Materials Research, Photonics Research Ontario, an Ontario Graduate Scholarship, the National Sciences and Engineering Research Council Canada, and Massey College. He is presently leading a research group innovating new enabling technologies for future photonic communication systems, devising improved approaches to the design of photonic systems and networks, and exploring novel materials and devices for photonics including polymers and photonic bandgap structures.

Genlin Tan received the engineering physics degree from Quinghua University, China, in 1961.

Since then, he has been engaged in teaching and research in the Department of Electrical Engineering, Beijing Polytechnic University, Beijing, China, where he was a Professor. His research concerns microcomputer application, integrated circuit analysis and optimization, semiconductor device simulation, and layout optimization of IC design. He is the author or coauthor of more than 40 articles and three books and acted as a reviewer for IEEE TRANSACTIONS ON ELECTRON DEVICES, IEEE JOURNAL OF QUANTUM ELECTRONICS, and *Applied Physics*. During 1987–1988, he was a Visiting Scholar in the Department of Electrical Engineering and Computer Science at the University of California at San Diego, La Jolla. Since 1989, he has been a Senior Research Associate in the Department of Electrical and Computer Engineering, University of Toronto, Ont., Canada. His current research interests include simulation and optimization of high-speed semiconductor devices, optoelectronic devices, and integrated circuits.

Jimmy M. Xu received the Ph.D. degree in electrical engineering from the University of Minnesota, Minneapolis in 1987.

Currently, he is a Chair Professor in the Department of Electrical and Computer Engineering, University of Toronto, Toronto, Ont., Canada, with the title of Nortel Professor of Emerging Technologies. He is the Director of the Nortel Institute at the University of Toronto and is a Principal Investigator of the Ontario Laser and Lightwave Research Centre. He is also a Principal Investigator of the Ontario Centre for Materials Research and a key associate of the Information Technology Research Centre. He has authored and coauthored more than 100 refereed papers in physics and engineering journals and more than 60 refereed conference papers. He has been granted ten patents on electronics and photonics devices. His current research interests include semiconductor physics, nanostructures, quantum electronics, and compound semiconductor device design, modeling, and measurements. Currently, he leads a group of 12 researchers and graduate students at the Optoelectronics Laboratory, University of Toronto, and conducts research primarily in the areas of optoelectronics, quantum electronics, nanostructure physics, heterostructure transistors, quantum-well electronics, and photonics devices, as well as large scale computer simulations. The Optoelectronics Laboratory is sponsored by Nortel and conducts research projects funded by agencies and companies in Canada, the United States, France, and Japan.

Prof. Xu was awarded the 1995 Steacie Prize for contributions to fundamental and applied quantum electronics, the 1995 Conference Board of Canada—NSERC Award for Best Practices in University–Industry R&D (Honorable Mention), and the 1996 FCCP Award of Merit for Outstanding Contributions in Science and Technology. One of his students received the NSERC Doctoral Thesis Prize (Engineering), another was given the Best Student Paper Award LEOS'94, and a third was awarded the Centennial Thesis Prize from the University of Toronto. He is a member of the IEEE Electron Devices Society Meeting Committee and an *ex-officio* member of the IEEE Electron Devices Society Administration Committee. He is an Editor of IEEE TRANSACTIONS ON ELECTRON DEVICES.